Iranian Journal of Chemical Engineering
Vol. 3, No. 3 (Summer), 2006, IAChE

Preparation of Lanthanum–Nickel–Aluminium Perovskite Systems and their Application in Methane-Reforming Reactions

*P. Moradi, M. Parvari**
Chemical Engineering College, Iran University of Science and Technology, Tehran, Iran.

Abstract

In this study we developed LaNixAl1-xO3 perovskite systems using a sol-gel method (with propionic acid as solvent) to use in methane-reforming reactions for producing synthesis gas. To understand the roles of the nature of the precursor and calcination conditions on the formation of LaNixAl1-xO3, we carried out identifications using NMR, FT-IR, XRD, SEM, and TEM. The precursor structure is a function of raw materials and calcination conditions. Nitrate salts of nickel, aluminium, and lanthanum, and calcinations at 750ºC for 4 h gave pure LaNixAl1-xO3 perovskite with good homogeneity, even at nanoscopic scales. These systems are highly efficient catalysts in steam and the dry reforming of methane. Various ratios of hydrogen to carbon monoxide in synthesis gas can be achieved by changing the feed type. We also investigated stabilization of these systems by studying the perovskite structure after reactivity tests. The optimum mixed perovskite for steam and dry reforming of methane is LaNi0.3Al0.7O3. The total conversion of CH4 is rapidly obtained at 750°C in steam reforming with a H2O/CH4 ratio = 3, the selectivity of CO is lower (55%) and the yield of hydrogen (98%) is higher compared to the ratio H2O/CH4 = 1. After 170 h of reaction, no deactivation had occurred, methane conversion remained higher than 90% at 750°C and in dry reforming, methane conversion and CO yield are about 98% and 95% respectively.

Keywords: *Nickel Perovskite, Methane Dry Reforming, Synthesis Gas*

Introduction

The conversion of hydrocarbons to hydrogen and carbon monoxide is important from an industrial point of view, and ranges from small hydrogen production units in fuel cells to large units in natural gas conversion to more easily-transported products and hydrogen plants in refineries [1]. Steam reforming of methane is an industrial process that produces synthesis gas with the highest H_2/CO ratio (≥ 3). The poor selectivity for CO due to the water-gas shift reaction is suitable for hydrogen plants [2].

Oxyreforming ($H_2/CO = 2$) and dry reforming ($H_2/CO = 1$) have been proposed as alternatives to achieve a high CO selectivity and a more appropriate H_2/CO ratio for methanol and Fischer-Tropsch synthesis. Due to the high level of carbon formation from methane and CO ($CH_4 \rightleftharpoons C + 2H_2$; $2CO \rightleftharpoons CO_2 + C$), dry reforming has not been widely used; however, dry reforming has attracted

* - Corresponding author: E-mail: parvari@iust.ac.ir

interest from both industrial and environmental perspectives. Both steam and dry reforming are highly endothermic and reversible. It is therefore necessary to operate at high temperatures to achieve equilibrium between methane, water, carbon monoxide, and carbon dioxide, together with the water gas shift reaction.

Catalysts that contain nickel are most commonly used because of their fast turnover rate, low cost, and relatively long-term stability [3]. Metal particles (Ni) are the active sites [4]; however, they tend to sinter under the reaction conditions. This in turn leads to a reduction in the number of active sites and an increase in carbon deposition [5,6]. Other metals such as cobalt, iron, and noble metals (Pt, Pd, Rh) have been tested as catalysts, especially in dry reforming [7,8, 9]. Supports such as CaO and MgO increase the stability and lifetime of the catalyst [10]. The addition of alkali earth or rare earth elements is important in reducing carbon deposition [11, 12]. To prevent the sintering of metal particles, dilution of nickel by a second metal such as Mn, Fe, Cu, or Al [13-17] is required. Perovskites (containing La, Ni, Fe or La, Co, Fe) have previously been constructed using the above approaches [15, 18, 19]; however, the total reduction temperature for bimetallic perovskites such as $LaNiO_3$ and $LaCoO_3$ is much lower than that of methane reforming. Hence, they are quickly and totally reduced and then act as supported metals [20]. Nickel or cobalt from the trimetallic perovskites (LaNiFe or LaCoFe) can be completely or partially reduced to form active metallic species [15, 21, 26] at a temperature close to the reforming temperature; this can create strong metal-support interaction through an appropriate activation. $LaFeO_3$ perovskite is never or seldom reduced on the catalysts to perform as a metal deposited in strong interaction on the structure.

Previous studies [15, 18, 19, 21, 22] have demonstrated that a solid solution of nickel or cobalt with a second metal (Fe) can increase the reduction temperature of $LaNi_xFe_{1-x}O_3$ and $LaCo_xFe_{1-x}O_3$ perovskites in the function of x values (550°C for $LaNiO_3$, 825°C for $LaNi_{0.3}Fe_{0.7}O_3$, and from 640°C to close to 900°C for $LaCo_XFe_{1-x}O_3$).

It has also been documented that the trimetallic LaNiFe structure is preserved during steam reforming (for x = 0.3) [21] and that the catalyst acts as Ni in interaction with LaNiFe. In this case, the strong interaction between nickel and the defined structure limits both metal crystallite growth and carbon deposition; steam reforming can therefore be performed at a lower steam/ methane ratio (1/1).

Trimetallic nickel perovskite is of interest in terms of the reduction temperature and ageing. Alpha alumina is the industrial support with a surface area that is similar to that of perovskite. Nickel and alumina can be combined during tests into nickel aluminate. In this study we prepared a perovskite that contains Ni and Al to test how combinations of these two elements are suitable for methane reforming reactions. We used a combination of X-ray diffraction (XRD), scanning electron microscopy (SEM), transmission electron microscopy (TEM), nuclear magnetic resonance (NMR), and infra-red (IR) to study the effect of raw material type and calcination conditions on the microstructure and catalytic behaviour of $LaNi_xAl_{1-x}O_3$ perovskites used in steam (with various steam/methane ratios) and the dry reforming of methane. Characterisation following tests provides information concerning the active phase of the perovskite during the reactivity test.

Experimental Section

Preparation of Catalysts

Preparation of catalysts was carried out via a sol-gel method using propionic acid as a solvent. Catalysts were prepared in accordance with the formula $LaNi_xAl_{1-x}O_3$, with x varying from 0.1 to 0.9 at intervals of 0.2, following the method developed in [15]

and [23]. Precursor solutions were prepared separately by dissolving raw materials in hot propionic acid. Nickel nitrate and acetate were used as nickel sources in different samples. Nitrate, oxide, or hydroxide was retained for lanthanum, while aluminium nitrate was used as an aluminium source. After dissolution into propionic acid, nickel and alumina solution were mixed and added to the lanthanum. After stirring for 30 minutes, the solvent was evaporated in a reflux process until resin formation. The resulting gel was calcined under increasing temperature at a rate of 3°C/min from 25°C to 750°C, and maintained at 750°C for 4 h. To determine the influence of calcination conditions, samples were calcined at various temperatures from 600°C to 1100°C. As the evaporation of solvent in the sol-gel method sometimes leads to the decomposition of nitrates and violent NO_2 production, a slow and controlled distillation of the solvent is recommended during this step. According to the explanations above, the effective factors affect the structure of perovskite and include the type of initial salts and calcination conditions that have been studied so different salts of Lanthanum, Nickel and Aluminium, five different reduction temperatures (600-1100 °C) and five catalyst composition ($0.1<x<0.9$) were used to prepare the samples in the present work.

Characterisation of the Gel

We undertook a study of precursors to determine the influence of the nature of raw materials on perovskite preparation and to select the most appropriate combination of raw materials.

We studied the structure of resins obtained during the gel formation process using NMR and FT-IR, and studied the formation of precursors in the propionic acid solution using various combinations of raw materials, according to [23]. The solution of corresponding propionate and propionic acid is concentrated and hence a counter-solvent (hexane) was added. After freezing (-10°C), the resulting crystals were analysed by FTIR (3 wt% in KBr matrix).

Characterisation of Resulting Oxide

Powder X-ray diffraction (XRD) data were collected using a Siemens D-500 diffracto-meter and Cu-Kα radiation for determining crystalline phases and calculating lattice parameters.

Morphological observations of calcined catalysts prepared at different temperatures from 600°C to 1100°C were undertaken using a JEOL JSM 800 SEM. The nano-scopic state of the catalyst and its homogeneity were determined from transmission electron microscopy (TEM) analysis using a TOPCON EM-002B apparatus coupled to an energy dispersive X-ray spec-trometer (EDS). Prior to analysis, powder of the catalyst was subjected to ultra-sonic waves in alcohol; one drop of the obtained suspension was then deposited on a carbon-coated 1000 mesh copper grid. The TEM, operating at 200 KV (point to point resolution of 0.18 nm), was equipped with an ultra thin window KEVEX EDX spectrometer.

Specific surface area measurements were carried out via the BET method based on the N_2 physisorption capacity at 77 K on a Coulter SA 3100 apparatus.

The total amount of carbon deposited on the catalysts during steam and dry reforming reactions was measured by elemental analysis.

Temperature programmed reduction (TPR) measurements were performed on a 100 mg sample placed in a U-shaped quartz reactor (6.6 mm ID) using a heating rate of 15°C/min from 25°C to 900°C. The reductive gas used during this procedure was a mixture of He and 3% H_2 (total flow 50 ml/min). A thermal conductivity detector was used to analyse the effluent gas after water trapping, and quantification of hydrogen consumption was carried out.

Reactivity of Steam Reforming of Methane

Catalytic tests during steam reforming were performed at atmospheric pressure with two different ratios of methane to steam ($CH_4/H_2O = 1$ and $CH_4/H_2O = 1/3$).

The reaction conditions were as follows: fixed bed quartz reactor (6.6 mm ID), weight of catalyst: 200 mg, total feed flow rate: 50 ml/min, carrier gas: Argon.

For the ratio $CH_4/H_2O = 1$, the flow rates of components were: CH_4: 5.85 ml/min; H_2O: 0.0047 ml/min; Ar: 38.3 ml/min. For the ratio $CH_4/H_2O = 1/3$, the flow rates of components were: CH_4: 4.176 ml/min; H_2O: 0.001 ml/min; Ar: 33.3 ml/min. The outlet gas was analysed using a micro gas chromatograph that is able to simultaneously analyse the remaining CH_4 and produced CO, CO_2, and H_2. The feed gas flow rate was adjusted by mass flow controllers.

The catalyst was heated to 750°C under the argon flow with a rate of temperature increase of 10°C/min. Methane (CH_4 flow: 4.1 ml/min) and water were then introduced to the reactor. The system was maintained at this temperature for ½ h, after which the temperature was changed in a program comprising four ramps. In the first ramp, the temperature was reduced stepwise to 550°C at 50°C increments, with GC analysis at each increment of temperature decrease. The second ramp involved a stepwise increase in temperature from 550°C to 800°C at a rate of 3°C/min, with GC analysis at every 50°C. The third and forth ramps were the same as the first and second, respectively, except that the temperature was reduced from 800°C at the end of the experiment. The catalyst was then rapidly cooled to room temperature.

As well as the prepared mixed oxide, we also tested a commercial catalyst (24.7 wt% Ni/α-Al_2O_3 from ICI SYNETIX) used in methane steam reforming plants for comparison.

To determine the lifetime of the prepared perovskite system, samples were tested in the steam reforming reaction with a feed ratio of $CH_4/H_2O = 1/3$ for approximately 170 h at 750°C.

Reactivity in the Dry Reforming of Methane

Operating conditions were as follows: fixed bed quartz reactor (6.6 mm ID); feed flow rates: CH_4: 5 ml/min, CO_2: 5 ml/min, Ar: 40 ml/min; weight of catalyst: 200 mg; inlet temperature: 350–800°C. The outlet gas was analysed simultaneously by two gas chromatographs, with one of the chromatographs measuring the amount of remaining methane and produced carbon oxide, and the other measuring the produced carbon monoxide and hydrogen.

The temperature program comprised an initial treatment and three cycles. The initial treatment consisted of a temperature increase from 25°C to 350°C at a rate of 10°C/min. During this step, no synthesis gas was produced for each catalyst. The first cycle was performed by a continuous temperature increase from 350°C to 800°C, increasing at 3°C/min; during this stage, chromatographic analyses were performed every 50°C until a 2-h stage at 800°C that involved three GC analyses. Finally, a stepwise decrease was undertaken at 50°C increments to 350°C with GC analyses at each stage. The sample was then kept for nearly 12 h under an argon atmosphere. The second cycle was similar to the first, except that the initial temperature was 350°C.

The third cycle involved a temperature increase up to 800°C. The catalyst was then cooled rapidly to room temperature. To determine the lifetime of the prepared perovskite system, samples were tested in a dry reforming reaction at 750°C for approximately 170 h.

Methane conversion, CO selectivity, and CO yield were calculated as follows:

CH_4 conversion = $(CH_{4in}\text{-}CH_{4out})*100/CH_{4in}$

CO selectivity = $CO*100/(CH_{4in}\text{-}CH_{4out})$

CO yield = $CO*100/CH_{4in}$

Results and Discussion

Characterisation of Precursor Solutions

The resulting NMR spectra of gels obtained from nitrate solutions in propionic acid show

a change in the peak positions of protons of the CH_3 and CH_2 groups (0.90 and 2.16 ppm, respectively, compared to 1.2 and 2.4 ppm for propionic acid), indicating reactivity between propionic acid and the starting nitrate salts. We undertook gel characterisation using FT-IR (Table 1). From lanthanum oxide, the addition of propionic acid gives a monodentate propionate (1560 cm^{-1}). With nickel acetate, a mixture of mono and bidentate propionate is obtained (1568 cm^{-1} and 1520 cm^{-1}, respectively); however, when nickel nitrate is used as raw material, the substitution of nitrate by propionate depends on the nature of the cation and its hydration rate. As shown in Table 1, nitrates are present on the coordination sphere of the cor-responding metallic cation, surrounded by a propionic acid molecule. Water molecules are characterised between 1600 and 1700cm^{-1} [24,25], probably derived from the starting hydrated salt. Nitrate and propionate peaks coexist for the three nitrate salts of La, Ni, and Al, even after a prolonged ageing of the gel (12 h).

Characterisation of the $LaNi_xAl_{1-x}O_3$ System prior to Catalytic Tests

The elemental composition in the series of $LaNi_xAl_{1-x}O_3$ perovskites determined by fluorescence always presents a good balance compared to theoretical values. BET surface areas of catalysts are between 12 m^2/g (x=0.1) and 6 m^2/g (x = 0.9) for calcination at 750°C. The surface area is slightly higher for calcination at 650°C (15 to 8 m^2/g, respectively).

XRD diagrams of the $LaNi_xAl_{1-x}O_3$ mixed oxide series (x = 0.1, 0.3, 0.5, 0.7, and 0.9) prepared by nitrate salts are shown in Figure 1a; only a perovskite phase is obtained. However, with increasing x values the structure peaks shift regularly between those of $LaNiO_3$ [14] and $LaAlO_3$ [11]. An enlargement of the area in the XRD diagram for 2θ between 32.0° and 33.5° shows this progressive shift (Figure 1b). For preparations made from nickel acetate instead of nitrate salt, the intensity of the main diffraction line decreases, and lanthanum oxide and aluminium oxide are formed separately. The trimetallic structure was not gained, but $LaAlO_3$ and $LaNiO_3$ structures were formed. We consider that the formation of trimetallic structure is directly related to the initial presence of nitrates and to competition between the formation of bimetallic ($LaNiO_3$ and $LaAlO_3$) and trimetallic perovskite.

The lattice parameter (a) has been calculated from the six most intensive diffraction lines, assuming a pseudo-cubic structure (Figure 2). It increases linearly with x between 3.78 and 3.84 Å, validating the preparation of the solid solution. The obtained curve enables us to determine the nickel content (x) of the perovskite and will be used as a calibration system to evaluate the possible migration of nickel out of the structure during the catalytic test.

Figures 3a and 3b show SEM micrographs of samples calcined at 650 and 750°C, respecttively. The catalyst calcined at 750°C has a smooth surface, which explains the lower BET surface area. The holes formed during calcination at low temperature by the decomposition of nitrates and the departure of NO_2. Hence, the presence of nitrate in the starting salt seems to be favourable for the generation of holes.

Electron dispersive X-Ray spectroscopy (EDS) coupled to TEM measurement was carried out on different points of the samples using a broad focus beam (200 nm) (1) to determine the mean element proportions of the sample and a small focus beam (14 nm) (2 to 5) to ascertain the homogeneity of the preparation (Figure 4a) for $LaNi_{0.5}Al_{0.5}O_3$. The combined XRD and TEM characterisation demonstrates the formation of a homogeneous La-Ni-Al solid solution.

Table 1. IR bands (cm^{-1}) of the $LaNi_xAl_{1-x}O_3$ gel prepared by nitrates salts versus values of x

Composition of the gel (x)	νsCO	νasCOO	δasCH_3	νsCOO	δasCH_3 and ν_3NO	ν_2NO
0.1	1710	1565	1464	1440	1380	830
0.3	1710	1564	1467	1438	1387	834
0.5	1720	1560	1462	1437	1387	835
0.7	1720	1563	1460	1437	1388	835

Note: The standard peaks are as follows:
Monodentate propionate: νasCOO ≅ 1570, νsCOO ≅ 1410
Bidentate propionate: νasCOO ≅ 1520, νsCOO ≅ 1420
Propionic acid: νsCO = 1710, δasCH_3 = 1468, δasCH_3 ≅ 1380
Nitrate: ν_3NO ≅ 1380, ν_2NO ≅ 830

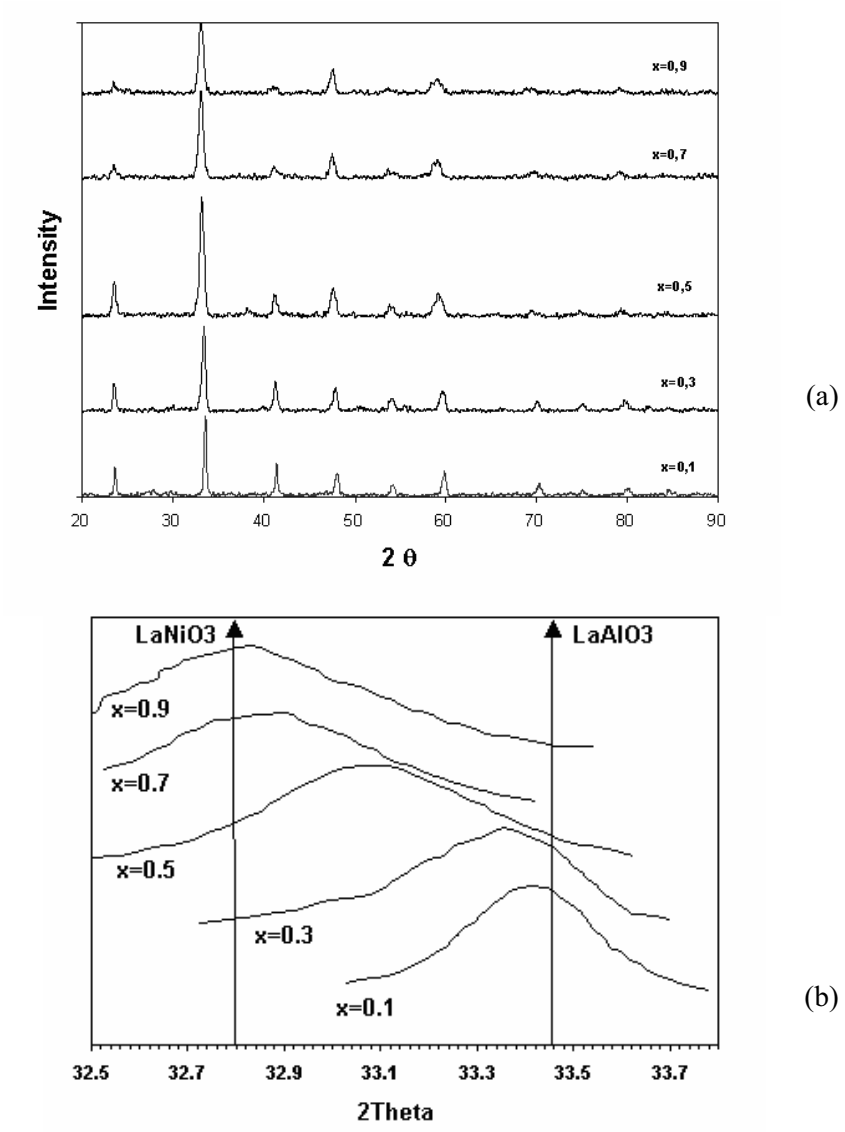

Figure 1. a) XRD diagrams for $LaNi_xAl_{1-x}O_3$ structures. b) Evolution of the position of the XRD highest peak

TEM micrographs (Figure 5) show a general view of the powders and a regular succession of atomic planes. The inter-reticular distances measured from the micrographs are very similar to lattice parameters calculated from XRD diagrams (3.789 Å compared to 3.796 Å).

Reducibility of the $LaNi_xAl_{1-X}O_3$ Perovskites

It is clear that the active species in methane reforming were reduced metal particles at the surface of the catalysts. It has also been suggested that strong interactions between reduced metals and defined structure is important to prevent sintering of metal particles. Accordingly, studies of the reducibility of metals is of prime interest. It has been previously demonstrated [15] that $LaNiO_3$ is reduced in two zones: at approximately 380°C with $La_2Ni_2O_5$ formation, and at 550°C with the obtention of Ni° particles deposited on La_2O_3. We studied the reducibility of LaNiAl perovskites and of Ni commercial catalysts (24.3 wt% Ni/α-Al_2O_3) following the procedure described above in the experimental section (Figure 6). $LaAlO_3$ is almost irreducible up to 800°C. The Ni perovskites have a first zone of reduction between 350°C and 380°C. This zone comprises two peaks or one peak and a shoulder. Figure 7 shows the evolution of the second reduction peak compared to the average temperature of the reforming reaction. The commercial catalyst is initially reduced slowly and continuously from 420°C until 750°C. A second zone of reduction is characterised at higher temperature between 620°C (x = 0.9) and 800°C (x = 0.1). The commercial catalyst is reduced at 780°C, close to the reduction temperature of $LaNi_{0.3}AL_{0.7}O_3$.

As demonstrated for $LaNi_xFe_{1-x}O_3$, the trimetallic perovskite structure always exists following the first reduction peak [18, 19]. The stability of the perovskite structure is shown with the second reduction peak. The temperature of the second reduction and the amount of consumed hydrogen, decrease with increasing the value of x. The high-temperature reduction peak characterises a strong interaction between Ni and the perovskite or the support. This strong interaction is probably one of the reasons for the good resistance to coking and the good ageing of the mixed La-Ni-Al perovskite catalysts.

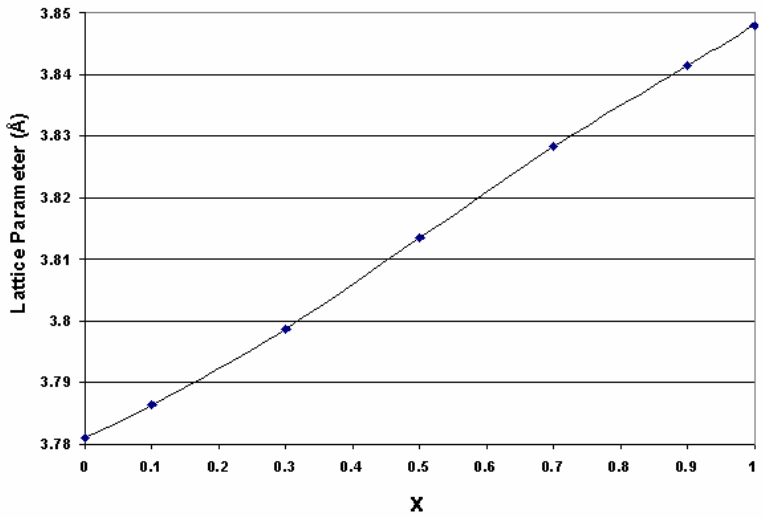

Figure 2. Evolution of the lattice parameter of the $LaNi_xAl_{1-x}O_3$ structures versus x

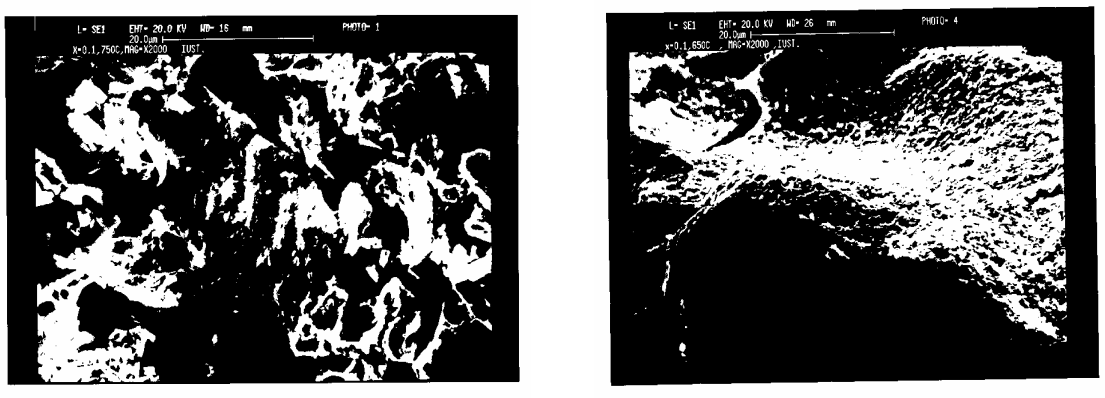

(a) (b)

Figure 3. SEM observations of the La-Ni-Al perovskite obtained from nitrate salts and calcined at a) 650°C and b) 750°C

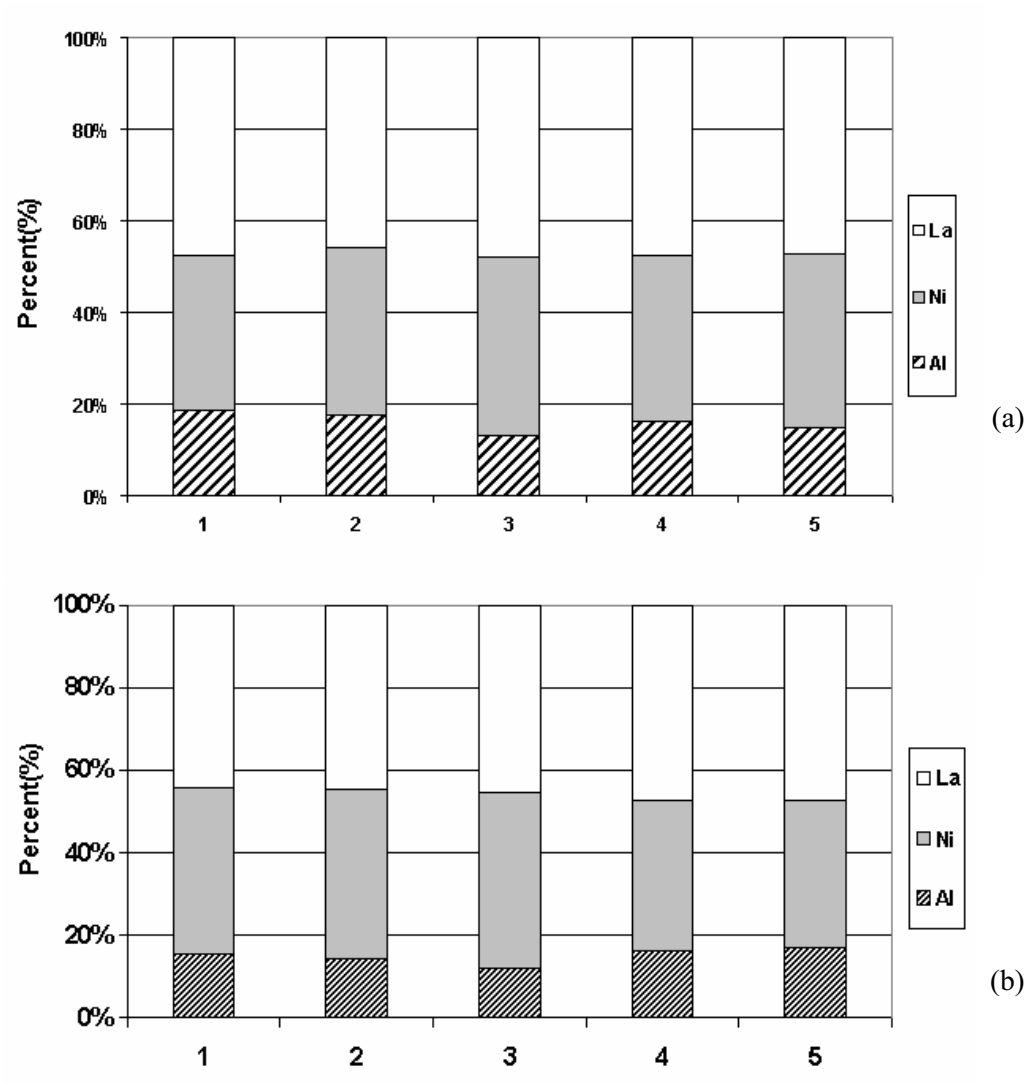

Figure 4. La, Ni, and Al distribution observed by EDS X-ray spectroscopy for LaNi0.5Al0.5O3 a) prior to the reactivity test and b) after steam reforming at 800°C with H2O/CH4 = 3

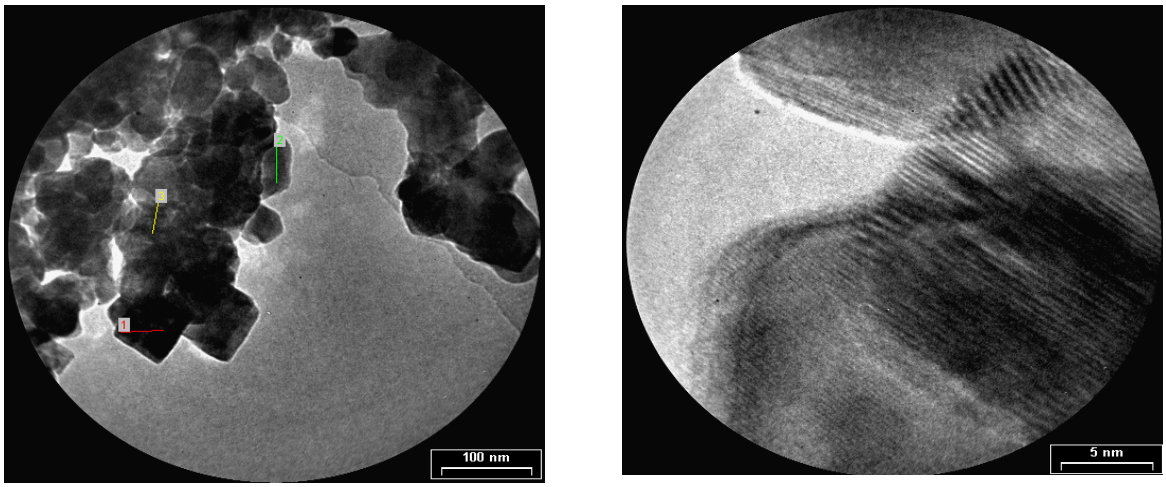

(a)

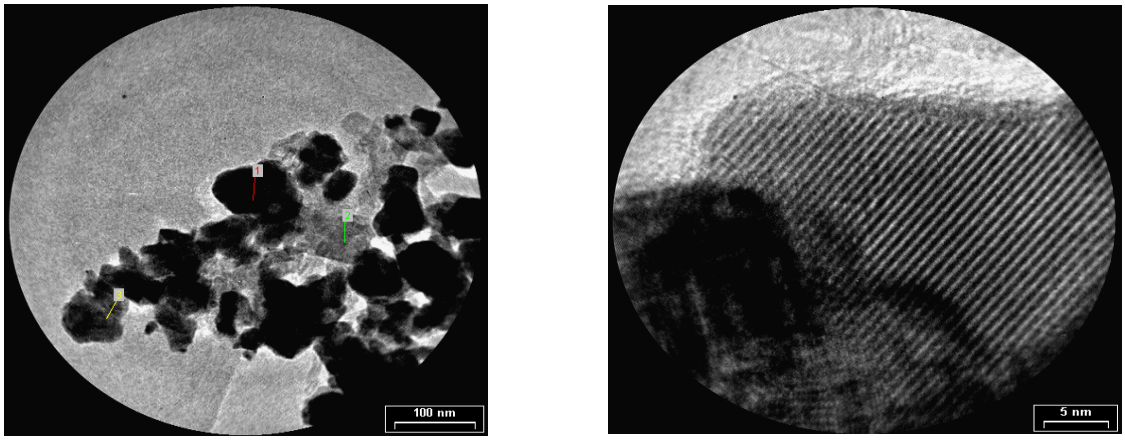

(b)

Figure 5. TEM analysis of $LaNi_{0.3}Al_{0.7}O_3$ a) prior to the reactivity test and b) after steam reforming at 750°C with $H_2O/CH_4 = 3$

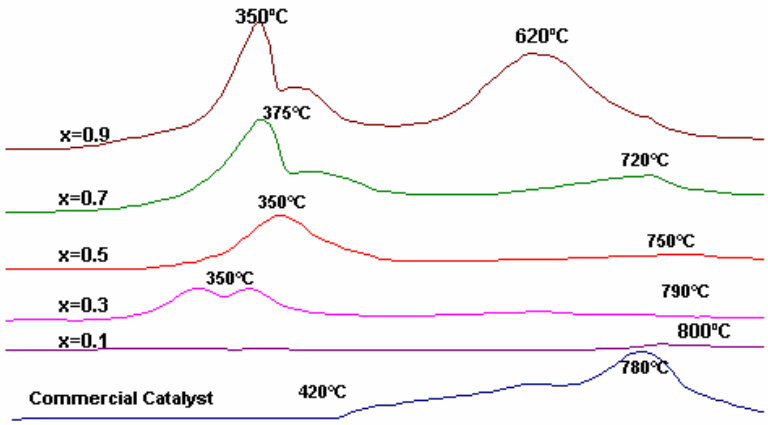

Figure 6. TPR curves of LaNixAl1-xO3 and 24.3 wt% Ni/α-Al2O3 commercial catalyst

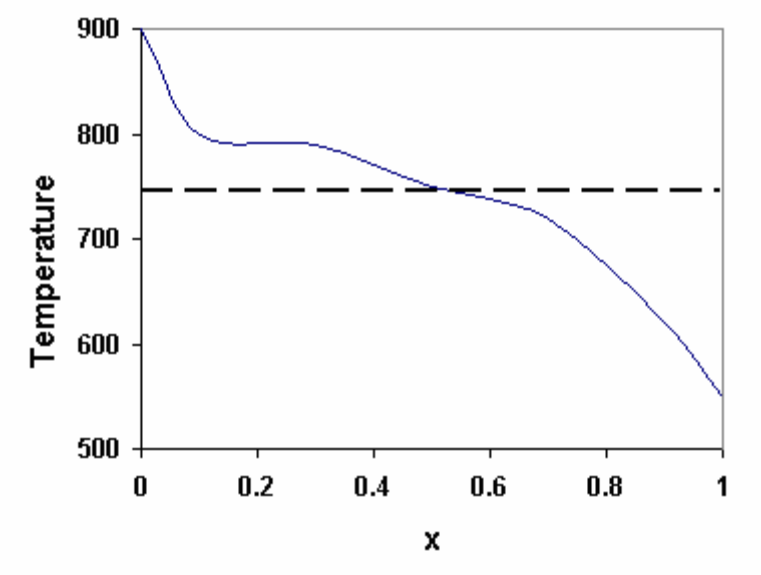

Figure 7. Temperature of the maximum consumption of hydrogen for the second reduction peak for $LaNi_xAl_{1-x}O_3$ and $Ni/\alpha\text{-}Al_2O_3$

Reactivity of $LaNi_xAl_{1-x}O_3$ in Methane Reforming

Study of Reactivity on Steam Reforming with $H_2O/CH_4 = 1$

During the third activation ramp (refer to experimental section), methane conversion is up to 80% at 650°C and reaches 100% at 800°C. Due to the low H_2O/CH_4 ratio, CO_2 formation is very low up to 700°C (Figure 8a). Hydrogen yield is up to 90% at 750°C (Figure 8b). The H_2/CO ratio decreased from 12 to 3 with increasing temperature; a H_2/CO ratio close to 3 is obtained at 750°C. Carbon formation for all catalysts is less than 2.5 wt% for all values of x except x = 1. Results are similar for the first and second ramps. As a comparison, for the 24.7 wt% $Ni/\alpha\text{-}Al_2O_3$ catalyst used at the same conditions, the reactor was blocked and filled by carbon after only 1 h of reaction. This is explained by the strong interaction of the free nickel obtained after reduction with the bimetallic $LaAlO_3$ perovskite. For $Ni/\alpha\text{-}Al_2O_3$, Ni is either free and able to produce nanotubes or nanofibers of carbon, or it is in too strong an interaction in the nickel aluminate structure. The catalyst with 0.9 Ni is less active than catalysts with a lower Ni content. This trend can be explained by progressive deactivation during the third ramp of reactivity, as previously described for LaNiFe perovskites [21, 22].

Study of Reactivity on Steam Reforming with $H_2O/CH_4 = 3$

When the $LaNi_{0.3}Al_{0.7}O_3$ catalyst was tested with a H_2O/CH_4 ratio= 3, the total conversion of CH_4 is rapidly obtained at 750°C (Figure 9). The selectivity of CO is lower (55%) and the yield of hydrogen is higher compared to the ratio H_2O/CH_4=1. After 170h. of reaction, no deactivation had occurred, methane conversion remained higher than 90% at 750°C, and carbon formation is less than 0.6 wt% of the starting catalyst. We also note that steam reforming of ethane occurred under both operating con-ditions. The conversion of C_2H_6 at 750ºC is 75%. The commercial catalyst performances are very similar to those of our sample, and no deactivation occurs with a water/methane ratio of three.

Study of Reactivity on Dry Reforming

In the dry reforming of methane, all catalytic

tests were performed following the same temperature program of two cycles and a third heating slope without previous reduction.

As indicated in Figure 10 methane is completely converted at 750°C, for $LaNi_{0.3}Al_{0.7}O_3$ in the second cycle. A change in the catalytic behaviour is observed between the first heating and cooling ramps. During the first heating ramp, CO production starts around 650°C, whereas it is still observed at the lower temperature of 550°C during the cooling ramp; this trend is related to reduction of the catalyst.

After activation of the catalysts, differences in the catalytic behaviours depend on x. At 800°C, the $LaNi_{0.1}Al_{0.9}O_3$ and $LaNi_{0.9}Al_{0.1}O_3$ systems give low CH_4 conversions (41.3% and 27%, respectively) and low CO yields (43.8% and 32.6%, respectively). For other catalysts, $0.1<x<0.9$, high activities are obtained at 800°C in the three cycles (Figure 11). The CO yields are above 95% for these perovskite systems; however, the activity of $LaNi_{0.5}Al_{0.5}O_3$ decreased after three days, related to approximately 8.76 wt% carbon deposition on this catalyst. This is also the case for catalysts with higher Ni contents. Likewise, carbon deposition for $LaNi_{0.3}Al_{0.7}O_3$ is around 1 wt%, and this catalyst shows very good activity and stability after one week of reaction at 750°C. The dry reforming of ethane performed well in the same conditions; total conversion of C_2H_6 is obtained at 650ºC.

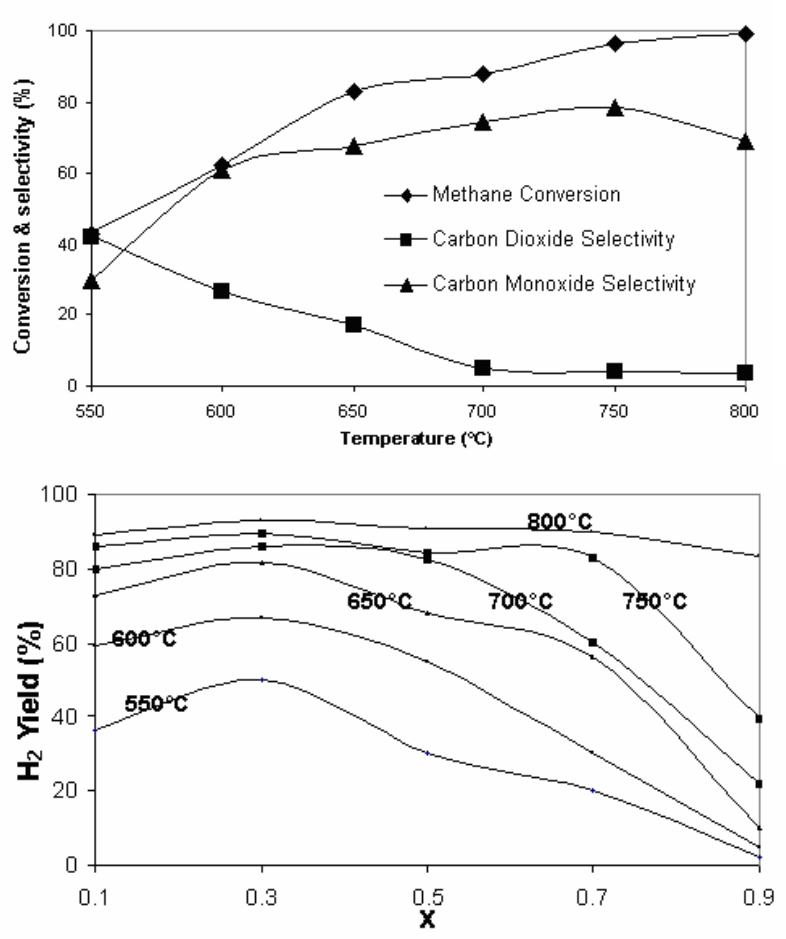

Figure 8. a) Methane conversion and CO2 and CO selectivities with a LaNi0.3Al0.7O3 catalyst. b) H2 yield in steam reforming (H2O/CH4 = 1) versus x at various temperatures

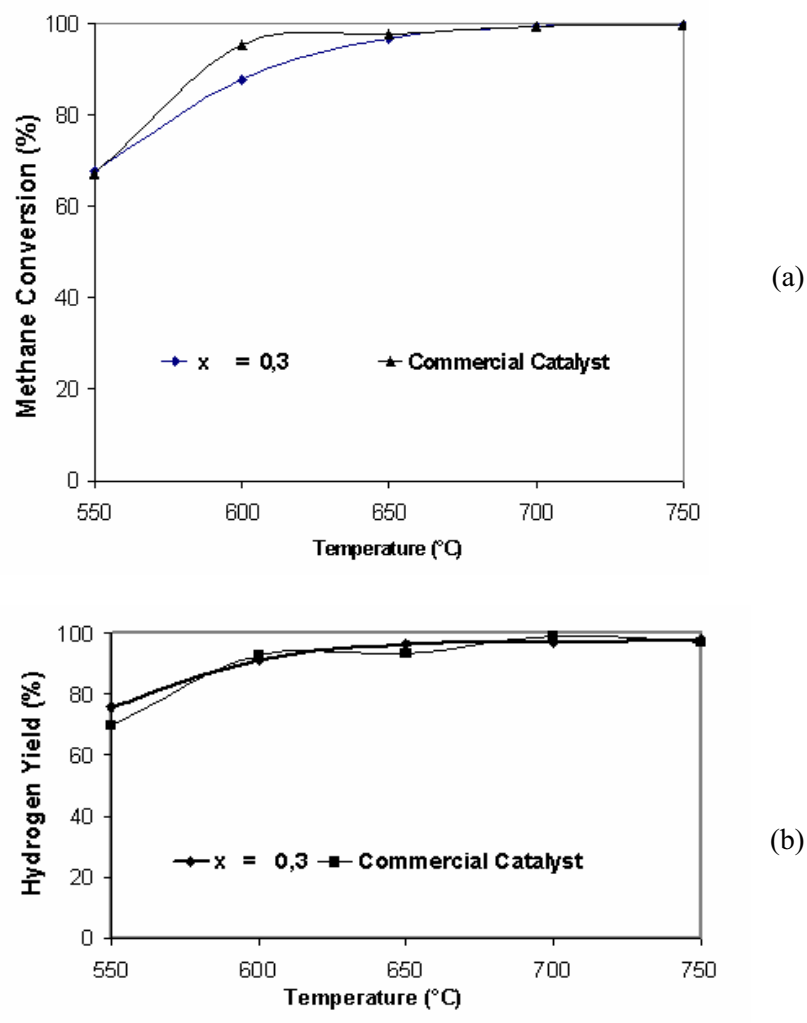

Figure 9. Steam reforming with H_2O/CH_4 = 3 for $LaNi_{0.3}Al_{0.7}O_3$ and 24.7 wt% Ni/α-Al_2O_3 commercial catalyst. a) Methane conversion. b) Hydrogen yield

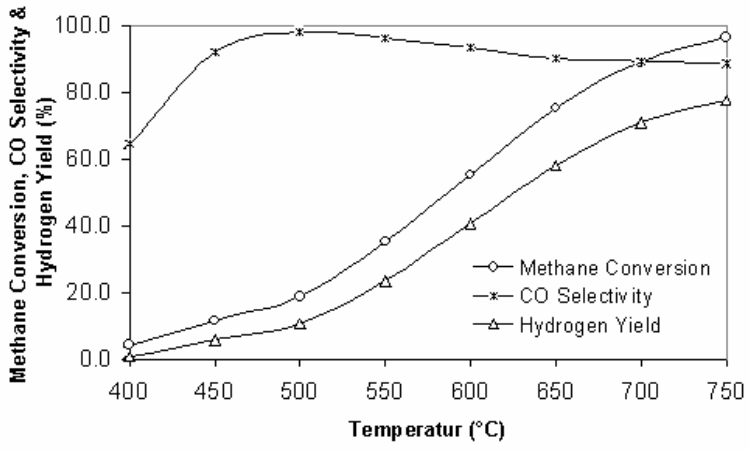

Figure 10. Methane conversion, CO selectivity, and hydrogen yield in the second cycle of dry reforming reaction for $LaNi_{0.3}Al_{0.7}O_3$

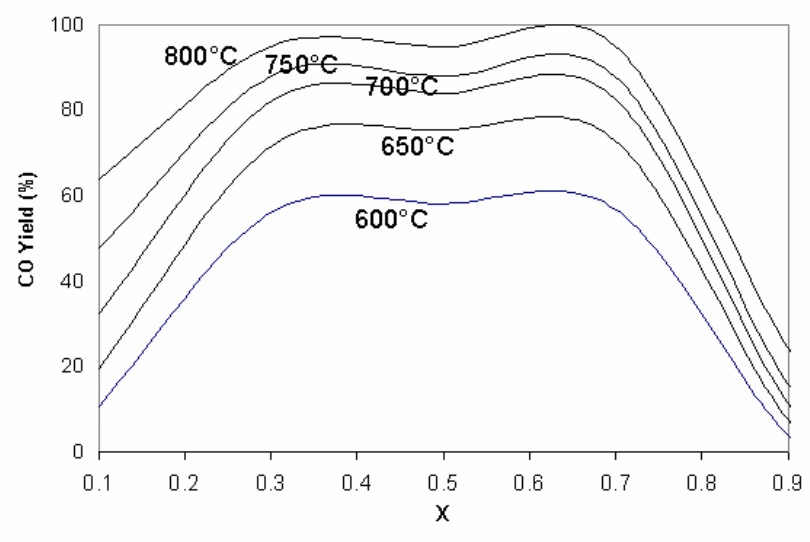

Figure 11. CO yields at various temperatures in the second cycle of dry reforming versus x

Characterisation of $LaNi_xAl_{1-x}O_3$ After Catalytic Test

To understand the evolution of the system during the test, the catalysts were characterised after the steam and dry reforming tests. After steam reforming, (H_2O/CH_4 = 3), LaNiAl catalysts show approximately the same XRD spectra as before the test except that some La_2O_3, $La(OH)_3$, or Lanthanum oxycarbonate could be characterised around 30º (2θ). Ni or NiO cannot be detected, showing apparently a great dispersion of the metal particles. A careful examination of the main diffraction peak for $LaNi_{0.3}Al_{0.7}O_3$ after a week of reactivity shows very few changes in the peak position; this indicates very good stability. Similar results have been obtained with the same catalyst after one week of reactivity in dry reforming; however, for x=0.7 after the same reactivity test, it is evident that the main peak is near 33.48º (2θ), corresponding to $LaAlO_3$ perovskite alone. La_2O_3 and $La(OH)_3$ are detected, but not Ni or NiO particles. We can conclude that the stability of the perovskite under the steam reforming conditions test depends on the amount of nickel incorporated in the initial perovskite. With a large amount of free nickel during the test, greater carbon deposition occurs.

EDS analysis confirms that the homogeneity of the catalyst after the test is similar to that of the catalyst before the test for x = 0.5. For x=0.7, parts with higher nickel concentrations being localised. We also measured the amount of carbon after the same test duration. The values are lower than 0.6 wt% of the total catalyst for all samples reacted in steam reforming with H_2O/CH_4=3 In steam reforming with H_2O/CH_4=1 and in dry reforming, carbon formation is higher (2.5 wt% and 1 wt%, respectively), as generally accepted.

Conclusions

We demonstrated that $LaNi_xAl_{1-x}O_3$ perovskites ($0<x<1$) obtained via a sol-gel related method are efficient in methane reforming (steam and dry reforming). We obtained solid solutions for all x values and a good homogeneity, especially if nitrate salts are used as precursors. The addition of aluminium to the $LaNiO_3$ perovskite structure generates a change in the temperature of nickel reducibility, stabilises the structure under reaction conditions, and limits the

migration of the active nickel; however, stability depends on the x value. The catalyst $LaNi_{0.3}Al_{0.7}O_3$ shows good stability and ageing in steam and dry reforming over 170 h. Few changes in structure were observed by XRD for this catalyst, but when the nickel content increases more nickel goes outside of the structure and the catalyst performs as Ni deposited on $Ni/LaAlO_3$.

Acknowledgements

The authors are deeply grateful to the Iranian Petrochemical Research and Technology Company for its financial support.

References

1. Rostrup-Nielsen, J. R., "New aspects of syngas production and use," *Catal. Today*, 63 (2-4), 159 (2000).
2. Rostrup-Nielsen, J. R., "Catalysis and large-scale conversion of natural gas ," *Catal. Today*, 21 (2-3), 257 (1994).
3. De Deken, J., Menon, P. G., Froment, G. F., Haemers, G., "On the nature of carbon in Ni/α-Al_2O_3 catalyst deactivated by the methane-steam reforming reaction," *J. Catal.*, 70 (1), 225 (1981).
4. Choudhary, V. R., Rane, V. H., Rajput, A. M., "Selective oxidation of methane to CO and H2 over unreduced NiO-rare earth oxide catalysts," *Catal. Lett.*, 22 (4), 289 (1993).
5. Kroll, V. C. H., Swaan, H. M., Mirodatos, C., "Methane Reforming Reaction with Carbon Dioxide Over Ni/SiO_2Catalyst: I. Deactivation Studies," *J. Catal.*, 161 (1), 409 (1996).
6. Bradford, M. C. J., Vannice, M. A., "CO_2Reforming of CH4over Supported Pt Catalysts," *J. Catal.,* 173 (1), 157 (1998).
7. Ashcroft, A. T., Cheetham, A. K., Green, M. L. H., Vernon, P. D. F., "Partial oxidation of methane to synthesis gas using carbon dioxide," *Nature* 352, 225 (1991).
8. Hickman, D. A., Schmidt, L. D., "Production of Syngas by Direct Catalytic Oxidation of Methane," *Science*, 259, 343 (1993).
9. Holmen, A., Olsvick, O., Rockstad, O. A., "Pyrolysis of natural gas: chemistry and process concepts," *Fuel Proc. Technol.*, 42 (2-3), 249 (1995).
10. Frusteri, F., Arena, F., Calogero, G., Torre, T., Parmaliana, A., "Potassium-enhanced stability of Ni/MgO catalysts in the dry-reforming of methane," *Catal. Comm.,* 2 (2), 49 (2001).
11. Slagtern, A., Olsbye, U., Blom, R., Dahl, I. M., Fjellvag, H., "In situ XRD characterization of La---Ni---Al---O model catalysts for CO_2 reforming of methane," *Appl. Catal. A*, 145 (1-2), 375 (1996).
12. Blom, R., Dahl, I.M., Slagtern, A., Sortland, B., Spjelkavik, A., Tangstad, E., "Carbon dioxide reforming of methane over lanthanum-modified catalysts in a fluidized-bed reactor," *Catal. Today*, 21 (2-3), 535 (1994).
13. Choi, J. S., Moon, K. I., Kim, Y. G., Lee, J. S., Kim, C. H., Trimm, D. L., "Stable carbon dioxide reforming of methane over modified Ni/Al_2O_3 catalysts," *Catal. Lett.,* 52 (1-2), 43 (1998).
14. Cheng, Z., Wu, Q., Li, J., Zhu, Q., "Effects of promoters and preparation procedures on reforming of methane with carbon dioxide over Ni/Al_2O_3 catalyst *Catal. Today,*" 30 (1-3), 147 (1996).
15. Provendier, H., Petit, C., Estournes, C., Libs, S., Kiennemann, A., "Stabilisation of active nickel catalysts in partial oxidation of methane to synthesis gas by iron addition," *Appl. Catal. A*, 180 (1-2), 163 (1999).
16. Bernardo, C.A., Alstrup, I., Rostrup-Nielsen, J.R., "Carbon deposition and methane steam reforming on silica-supported Ni---Cu catalysts," *J. Catal.,* 96 (2), 517 (1985).
17. Alstrup,I., Tavares, M. T., "Kinetics of Carbon Formation from CH4 + H2 on Silica-Supported Nickel and Ni-Cu Catalysts," *J. Catal.*, 139 (2), 513 (1993).
18. Rodriguez, G., Roger, A. C., Bedel, L., Carballo, L., Kiennemann, A., in: A.C.S. Symposium SERIES No. 852 Utilisation of Greenhouses Gases, C.J. Liu R.G. Mallinson, M. Aresta Eds., 2003,

Chapter IV, pp. 69-83.

19. Bedel, L., Roger, A. C., Kiennemann, A., Estournes, C., "Co^0 from partial reduction of $La(Co,Fe)O_3$ perovskites for Fischer–Tropsch synthesis," *Catal. Today*, 85 (2-4), 207 (2003).
20. Moriga, T., Usaka, O., Jmamura, T., Nakabayashi, I., Matsubara, I., Kinouchi, T., Kikkawa, S., Kanamaru, F., *Bull. Soc. Chim. Japan,* 67, 687 (1994).
21. Provendier, H., Petit, C., Kiennemann, A., "Steam reforming of methane on $LaNi_xFe_{1-x}O_3$ ($0 < x < 1$) perovskites," *C.R. Acad. Sci. Ser. C,* 4 (1), 57 (2001).
22. Provendier, H., Petit, C., Estournes, C., Kiennemann, A., "Synthesis and Characterization of LaNiO, LaNiFeO and LaNiCoO," *Stud. Surf. Sci. Catal.*, 107, 107 (1997).
23. Roger, A.C., Petit, C., Kiennemann, A., "Effect of Metallo-organic Precursors on the Synthesis of Sm–Sn Pyrochlore Catalysts: Application to the Oxidative Coupling of Methane," *J. Catal.,* 167 (2), 447 (1997).
24. Pitchon, V., Primet, M., Praliaud, H., "Alkali addition to silica-supported palladium: Infrared investigation of the carbon monoxide chemisorption," *Appl. Catal.B*, 62 (1), 317 (1990).
25. Cernák, J., Chomic, J., Kappenstein, C., Brahmi, R., Duprez, D., "Copper-zinc oxide catalyst. Part II. Preparation, IR characterization and thermal properties of novel bimetallic precursors," *Thermochim. Acta*, 276, 209 (1996).
26. Bedel, L., Roger, A.C., Rehspringer, J. L., Zimmermann, Y., Kiennemann, A., "$La_{(1-y)}Co_{0.4}Fe_{0.6}O_{3-\delta}$ perovskite oxides as catalysts for Fischer–Tropsch synthesis," *J. Catal.*, 235 (2), 279 (2005).